Influence of Time Dependent Material Properties in the Construction Stage Analysis of Composite Cable-Stayed Bridge

Bhupendra Prasad Mishra
Indian Institute of Technology Roorkee, Uttarakhand, India
Email: bhupendra_pm@ce.iitr.ac.in

Abstract

This study analyzes recent advancements in the erection analysis of cable-stayed bridges with composite steel–concrete decks, focusing on time-dependent effects during staged construction. While prior studies have addressed erection strategies, this work emphasizes the practical modeling of de-stressing and re-stressing operations using both backward and forward analysis methods. A parametric investigation quantifies the influence of creep and shrinkage on internal forces, showing that neglecting these effects can lead to camber deviations of up to 15 mm and cable force variations of 8–12%. The study demonstrates that incorporating accurate time-dependent material models is essential to control deflections and ensure structural performance. Findings reinforce the importance of detailed construction-stage analysis especially in cantilever erection methods to mitigate long-term deformation and associated economic implications. This research contributes practical insights for refining erection simulations and improving predictive accuracy in cable-stayed bridge design.

Keywords: Cable-stayed bridge, construction stage, time dependent material properties, creep, shrinkage, midas analysis, cantilever construction

Introduction

A civil structure, like a cable-stayed bridge, needs independent but connected studies for the finished structure and temporary structures throughout the construction. Each temporary construction at a certain stage of development has an impact on the succeeding stages. Additionally, it is normal practice to set up and take down temporary supports and wires while working on a project. Due to the variable maturities of adjacent parts, the structure continuously changes or develops as the construction process goes on. This causes changing material characteristics, such as modulus of elasticity and compressive strength. Due to fluctuating time-dependent qualities including concrete creep, shrinkage, modulus of elasticity (ageing), and tendon relaxation, structural behaviors like deflections and stress re-distribution continue to alter both during and after construction (Arzoumanian et al., 2016). The design of some structural components may be regulated during construction because the structural configuration varies continually in response to various loads and support circumstances and because each construction stage influences the phases that follow it. Since each step of the construction must be examined, it is necessary to conduct a time-dependent construction stage analysis. Without it, the analysis of the final stage alone would not be accurate (Cluley & Shepherd, 1996). Cable-stayed bridges can be categorized as medium-span and long-span bridges. In the past, medium-span cable-stayed bridges were often constructed for aesthetic rather than technological reasons. However, technological advances in building processes have increased their cost efficiency. Temporary support, rotation, or gradual launching may all be used to build medium-span cable-stayed bridges (Chen & Duan, 2014). In contrast, cable-stayed bridges have achieved great success in the construction of long-span bridges. For lengthy cable-stayed bridges, the cantilever approach is a feasible and cost-effective alternative. This method involves constructing segments and supporting them with new cables to balance their weight.

This study investigates the cantilever construction method for cable-stayed bridges, with a particular focus on enhancing the accuracy of construction-stage analysis. While the choice of construction technique generally depends on factors such as span length, structural configuration, and site conditions, a significant gap exists in the integration of backward and forward erection analysis with the time-dependent effects of creep and shrinkage in composite steel–concrete decks. This lack of integration often results in inaccuracies in camber predictions and internal force estimations during staged construction. To address this issue, the present study proposes an integrated analytical approach that considers both erection sequences and material time effects, aiming to improve the reliability of construction simulations and promote more efficient and accurate design practices for long-span cable-stayed bridges.

Construction on Temporary Supports

This style of construction allows the girder to be built continuously from one end to the other as shown in figure 1. The method produces precise control over the cable tension and geometry (Chen & Duan, 2014). The requirement for interim supports is the disadvantage. In many cases, it is not cost-effective to install temporary supports, usually over a high-water depth in the main bridge, which renders the process itself impracticable (Gautam, 2019).

Figure 1

Construction on temporary supports (Gimsing & Georgakis, 2011)
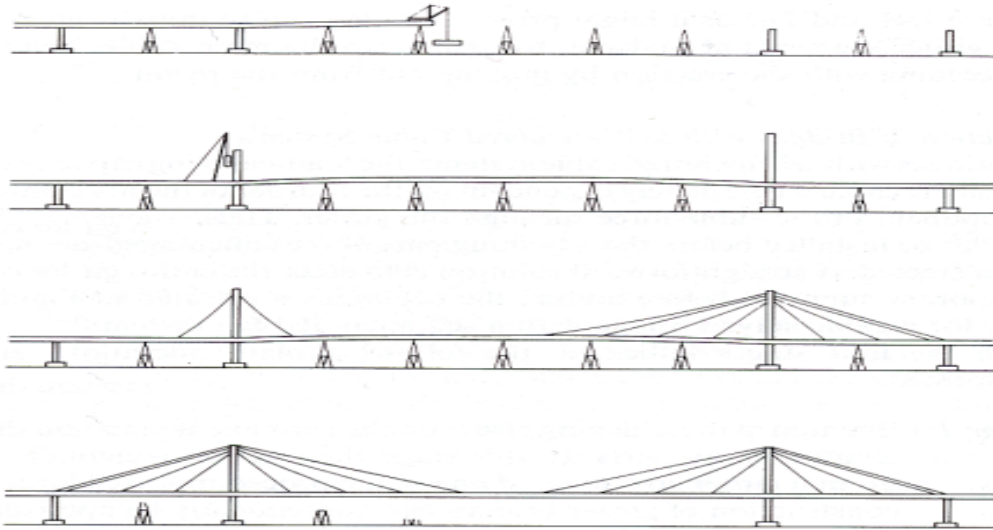
Construction by Rotation

Structural rotation is a construction approach that allows structures to be installed without interfering with traffic (road or river). The construction is constructed parallel to the road or river to be spanned and then rotated into its final position. During operation, the structure is supported by specific bearings (Chen & Duan, 2014). The erection process has a large impact on the foundation and pylon design. Because of the rotating process, excessive out-of-center forces creating large bending moments in the footing must be avoided. Bridge constructed by rotation method is shown in figure 2.

Figure 2

Bridge Construction by rotation (https://www.freyssinet.com)


Construction by Incremental Launching

Leonardt's incremental launching method, first in 1961, has been extensively employed in bridge construction. With this technique, the superstructure is cast or partially built at a fixed place behind one of the abutments. Subsequent segments are cast and added to the already-positioned piece after the finished or nearly finished section is horizontally pushed into position as in figure 3. Benefits of this technique include the removal of the requirement for bulky erection tools and falsework. To lessen the cantilever moment throughout the procedure, a light steel truss serves as the launching nose (Gautam, 2019). The incremental launching technique is often used in the main span of cable-stayed bridges and may be used to steel or composite decking. It is appropriate for small and medium-sized cable-stayed bridges, and it is especially advantageous for intermediate piers in the side span. In the main span, however, temporary supports are necessary. Once the construction is complete, all of the stays may be tensioned at the same time. If the deck is hung using cables attached laterally to the deck, adopting the gradual launching technique may provide a hurdle. In such instances, the anchor blocks on both sides of the deck enlarge the deck, possibly causing transversal stresses in the columns of a pylon constructed of two vertical columns beyond the extended deck width. To address this, bracing between the columns becomes necessary. Alternatively, for pylons shaped like inverted V or Y, the necessary space for the deck can be designed into the pylon.

Figure 3

*Construction by incremental lunching (Chen & Duan, 2014)*
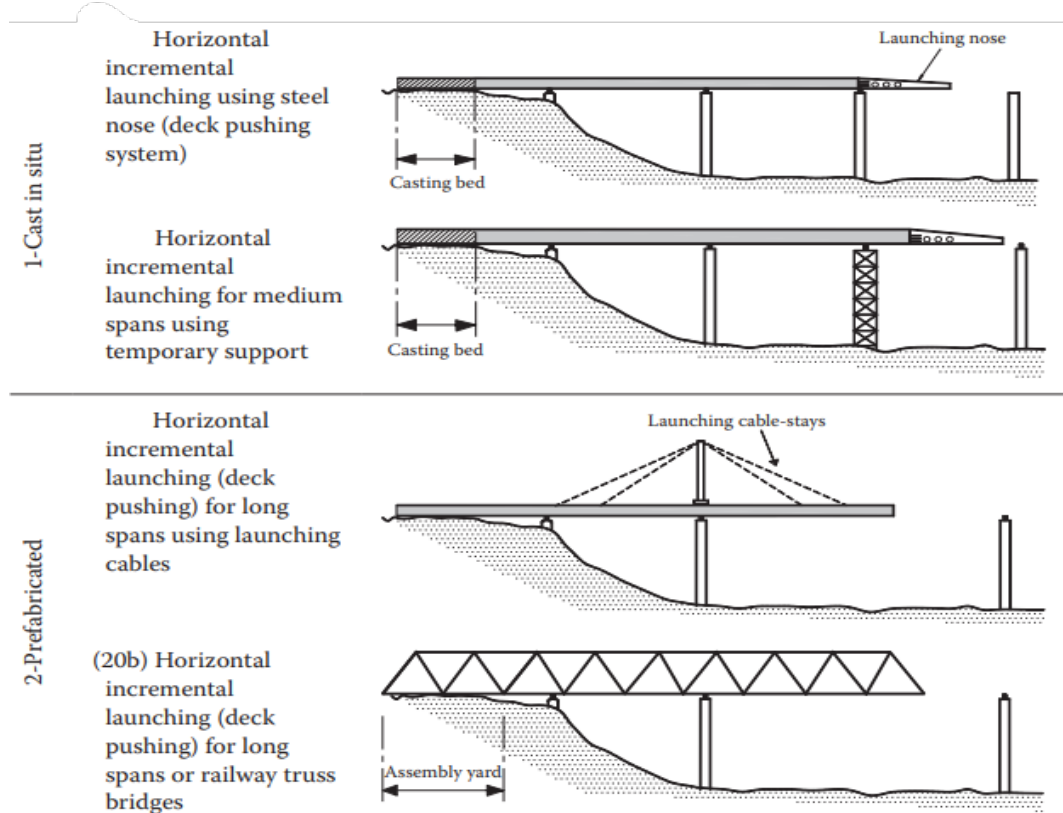
Construction by Cantilever Method

   The superstructure is built in segments utilizing two form travelers, one on each side of the bridge superstructure. When there are barriers on the ground, this strategy is applied (Chen & Duan, 2014). Temporary supports can be completely omitted in a traditional three-span bridge if the superstructure is built using the free-cantilever approach. A typical example of construction by cantilever method is present in figure 4. In a cable-stayed bridge, the selection of cable anchor points is critical to allowing unrestricted cantilevering of the stiffening girder from one anchor point to the next without the need of temporary supports. When new segments are added to extend the cantilever arms, the structure must be able to endure unsymmetrical construction forces (Pipinato et al., 2012). Dynamic forces, such as those caused by the fall of a mobile carriage, and wind effects also need to be considered, as they can significantly impact the temporary configuration. In some cases, seismic effects may also be taken into account during the construction period (Svensson, 2012). The specific issues encountered during construction depend on the connection between the deck and the pylon. While

rigid connections between the deck and pylon can limit construction problems, fixed connections are less common in cable-stayed bridges due to thermal effects. Instead, the deck is often supported just by the pylon or not supported at all. In such circumstances, a temporary connection between the girder and a support must be constructed. This support may be the pylon itself, or if the deck is near to the ground, a separate temporary construction distinct from the pylon. By using elastic connections, such as neoprene bearings, the deck can be supported by the pier to handle transverse bending moments while still allowing longitudinal deformations.

Figure 4

Construction by cantilever method (Gautam, 2019)
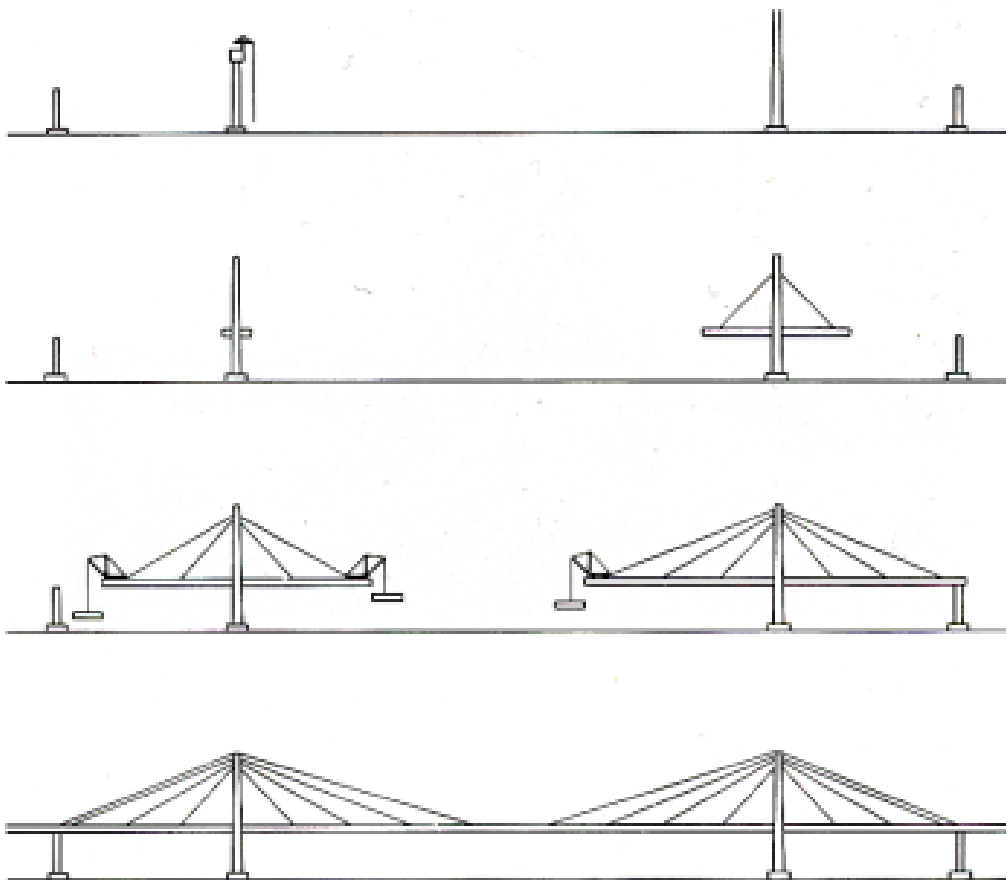
Construction of Pylon

The choice of material and construction methods for pylons in cable-stayed bridges greatly depends on the size and height of the structure. Steel pylons, commonly found in moderate-sized bridges, can be erected using mobile or floating cranes. Advancements in

floating crane technology have allowed for the efficient erection of complete steel pylons in one or two pieces. For taller pylons, a climbing crane that follows the pylon's growth is often employed. On the other hand, concrete pylons offer their own set of construction options. Slip-forming, which involves continuous casting of concrete, is favored for pylons built on land with easy concrete access. Climbing scaffolding is used when casting the pylon legs away from the coast, where all concrete must be transported by sea (Gimsing & Georgakis, 2011). During the construction of cable-stayed bridges with A- or diamond-shaped pylons, additional temporary struts are installed between the legs to address significant bending moments. Wind-induced oscillations pose a concern during construction, particularly for steel pylons due to their lighter mass and higher flexibility. Wind tunnel tests are commonly conducted to assess the stability of free-standing pylons. Concrete pylons benefit from the pre-stressing effect of the cable system, resulting in a lower requirement for vertical reinforcement in the completed structure. Therefore, careful consideration and control of all structural parts are crucial throughout the construction process (Gautam, 2019). In summary, the choice between steel and concrete pylons and the corresponding construction methods depend on factors such as bridge size, height, and site conditions. The erection process involves the use of cranes, including mobile, floating, and climbing cranes, to lift and position the pylon components. By implementing appropriate construction techniques and conducting thorough assessments, cable-stayed bridge pylons can be safely and efficiently constructed to support the overall bridge structure.

Construction of Deck

In Particular, for the construction of cast-in-place decking for cable-stayed bridges a movable carriage carries the weight of fresh concrete for each new section. However, traditional mobile carriages can create unfavorable temporary bending moments in the deck, which can be a concern, particularly when the deck has limited inertia. To mitigate this issue, the distance between the cables can be reduced, and the mobile carriage design can be improved to allow for cable tensioning before moving the carriage. Another option is to use a cable-stayed mobile carriage, either with temporary cables or final cables, which provide stability and allow for the concreting of longer segments. These methods allow for the building of flexible decks with minimal bending moments and the placement of tendons at the appropriate phases. Careful consideration of stay forces and anchoring methods is essential to ensure the integrity of the structure during construction. By employing these techniques, the construction of cable-stayed bridge decks can be optimized, addressing the challenges associated with temporary bending moments and limited deck inertia.

Concrete Deck. Precast segmental bridges offer economic advantages for larger

bridge projects, where the costs associated with setting up a casting yard can be offset by the speed of segment casting and the efficiency of the erection process. This approach becomes particularly appealing when pre-fabrication is utilized for both the main and side spans of the bridge. Examples of such projects include the Sunshine Skyway Bridge in Florida, where uniform cross-section segments weighing 120 tons were precast nearby and transported by barges for installation, and the James River Bridge in Virginia, which employed twin parallel precast box girders connected by transverse frames (Chen & Duan, 2014). According to Virlogeux (Gautam, 2019), cast-in-situ construction methods are advantageous for cable-stayed bridges as they allow for limited tensile stresses during erection. This approach ensures that the bridge is in optimal condition to handle limited live loads without subjecting the concrete elements to tensile stress. In cases where partially prestressed concrete members are needed to balance extreme live loads, precast segments may not be suitable due to their lack of flexibility. Therefore, the choice between cast-in-situ and precast construction methods depends on the specific bridge design, desired construction speed, and the ability to accommodate varying load conditions (Purohit & Bage, 2017).

Composite/Steel Deck. Derrick cranes, sometimes known as floating cranes, are often employed to build steel and composite decking in cable-stayed bridges. However, standard derrick cranes have limited lifting capacity, usually not exceeding 200 tons (Gimsing & Georgakis, 2011). To accommodate this, smaller erection units are used, resulting in more erection joints. In some cases, the girder needs to be divided both transversally and longitudinally to ensure each segment remains within the lifting capacity of the cranes. Attention must be given to the high bending moments generated during lifting operations when determining segment sizes. Cables are then fitted and tensioned, enabling the derrick to advance onto the freshly installed section in preparation for raising the next one. When compared to all-concrete decks, composite cable-stayed bridges with a steel girder and a concrete deck offer a lighter construction. The steel parts are prefabricated with stringent quality control, while the concrete deck serves as the highway and bears the majority of the axial stress of the cables. Construction of a composite deck involves building the steel structure segment by segment, suspending it from the cables, and subsequently casting or installing the concrete slab in segments. Maintaining a distance of two or three segments between steel and concrete operations allows for independent progress (Svensson, 2012).

During the initial tensioning stage of a composite deck, the steel structure of a new segment can experience upward or downward bending depending on the applied cable force. These deformations become fixed once the concrete is cast on top, preventing the deck from assuming its undesired final shape. To correct this, additional bending would need to be applied to force the deck into the correct shape, resulting in non-ideal dead

load moments for the continuous beam. To address these challenges, a two-step cable tensioning sequence is typically employed in the erection process. In the first tensioning stage, the cable force is chosen to minimize the locked-in curvature and associated creep effects. By carefully shaping the steel beam to include equal amounts of positive and negative bending, a straight deck can be achieved. The resulting concrete creep effects are then counteracted by the subsequent straightening of the steel, ensuring their opposing influences negate each other as shown in figure 5. This approach helps to optimize the final shape of the composite deck while mitigating the detrimental effects of curvature and creep (Schlaich, 2001).

Figure 5

Construction methods for construction of the composite cable-stayed bridge (Schlaich, 2001)
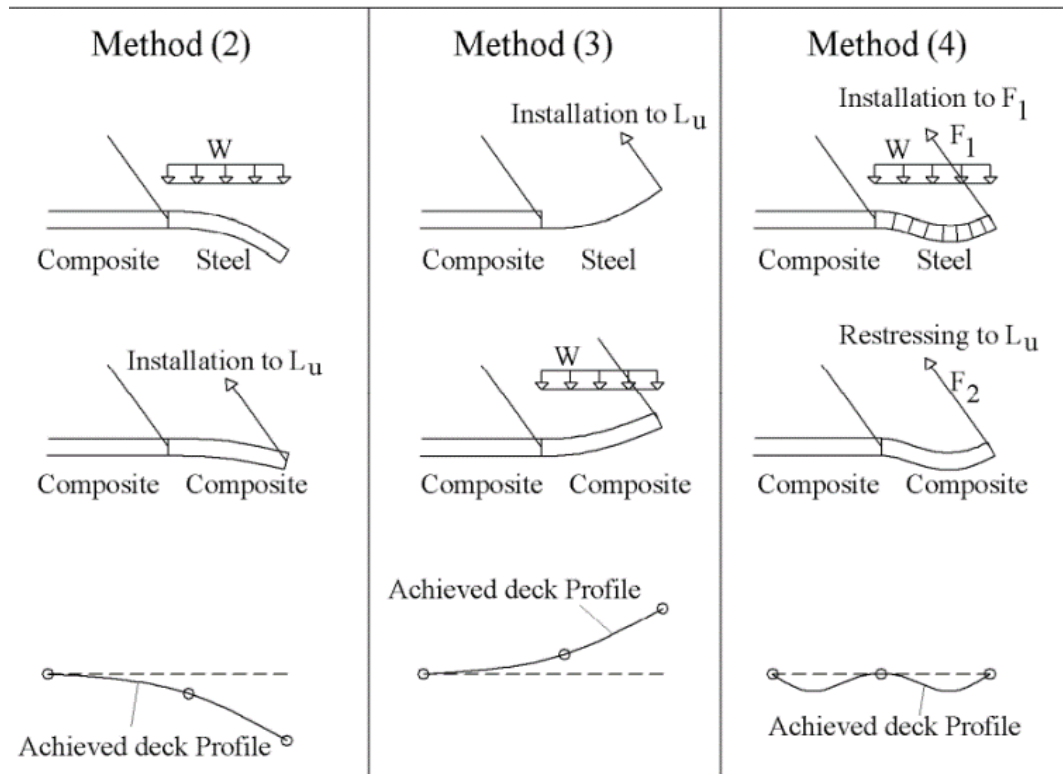
The structural design of a cable-stayed bridge can vary significantly depending on how it is constructed. In this regard, the construction phases should be organized so that they include those that have an impact on the structural system and are used to evaluate structural safety (Kim et al., 2017). It is known as forward analysis when the analysis is carried out after the erection sequence to achieve this goal. Stresses in the various phases of construction, the order of the stages, and the feasibility of building may all be

examined through the forward analysis, and the best construction strategy can then be chosen.

Construction Stage Analysis and Results

Midas civil is a comprehensive analysis program designed for modelling and analysing structural systems, with a focus on civil structures like box girder or composite bridges. It offers specialized features tailored to the analysis of such structures, including Construction Stage Analysis. Users may establish construction phases by adjusting the structural system, allowing the addition or removal of parts, changes in boundary conditions, and the activation or deactivation of loadings to imitate actual situations throughout each construction stage.

Figure 6

Flow Chart for performing construction stage analysis in midas civil
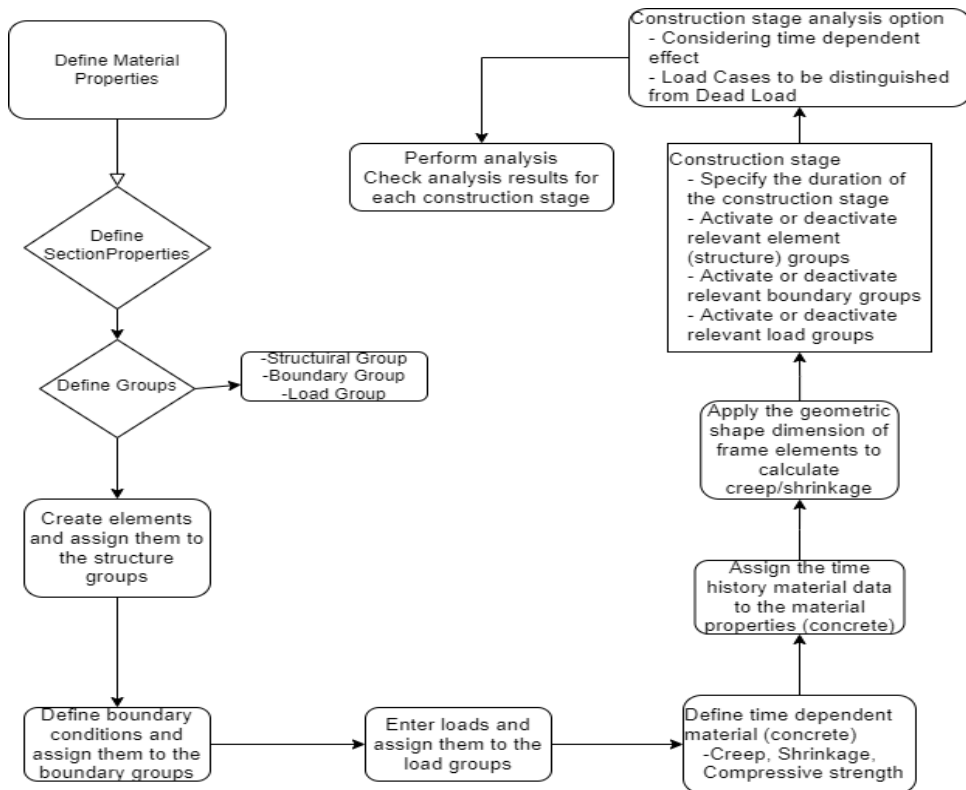
The tool can properly analyse structure erection and dismantlement by integrating time steps to reflect loading and unloading periods within a construction stage without causing structural system changes. To model structural systems, midas civil provides various element types, including General Beam elements, Truss elements, Tension-Truss
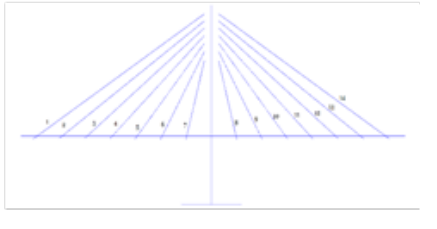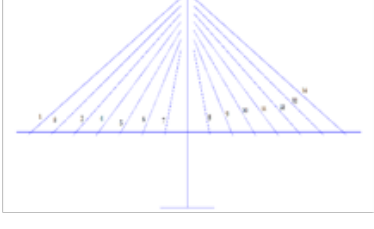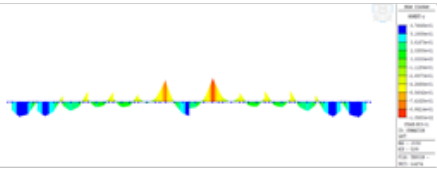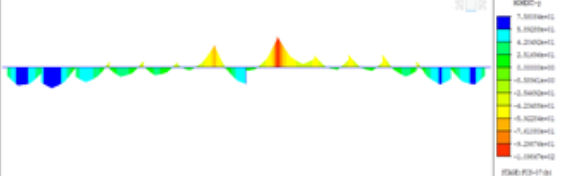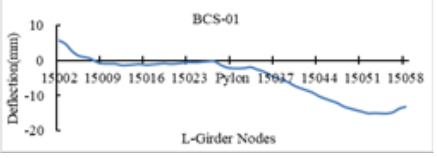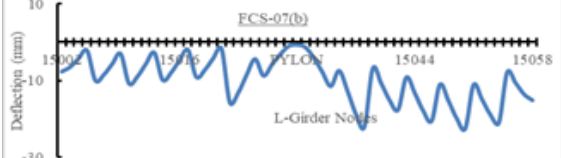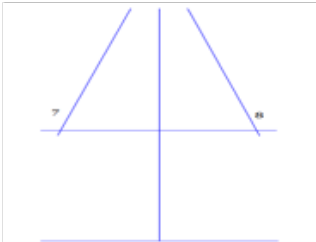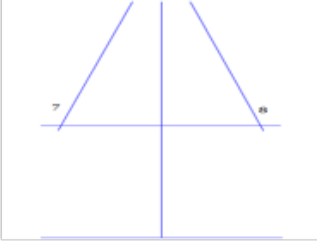
Cable elements (catenary cable element), as well as plate and shell elements. It allows for the calculation of initial pre-stressing forces through equilibrium optimization, primarily in linear analysis scenarios where different loadings can be superposed. The program utilizes the Unknown Load Factor function and initial equilibrium state analysis to determine the initial cable pre-stressing forces in completed cable-stayed bridges. midas civil can perform both linear and nonlinear static system evaluations using truss and cable components. P-delta effects and large displacement studies may be used to account for geometric non-linearities. Furthermore, the software makes it easier to incorporate structural non-linear behaviour during the building stage analysis, allowing for significant displacement studies and the modelling of material behaviours like creep and shrinkage. The steps for construction stage analysis in midas civil are given below.

Forward Method = Backward Method

The findings of the forward and backward assessments are equivalent as long as no creep or shrinkage is taken into account in the computation. Before the elements are deactivated, the backward approach requires that they be in a stress-free environment. It is necessary to move or balance loads until the reaction drops to zero before removing a support. A portion can be removed by first applying its weight upward to create a zero-stress condition (Gautam, 2019). All previous stage results are collected and applied to the current step in midas civil. Activated elements, boundary conditions, and loads stay active until they are disabled (Midas Bridge, n.d.).The neighboring remaining elements experience internal forces acting in opposite directions when an element is removed. Therefore, applying the loads in the opposite direction before removing the loads or elements is not necessary in midas civil. Forward and backward analyses yield different outcomes when used directly. The forward technique immediately breaks every junction between two pieces (Midas Bridge, n.d.). The backward technique assumes that the new segments are tangentially added to the preceding stage. As a result, there are discrepancies in the deformed shape when comparing the two results. Because the internal forces are unaffected by this scenario, the moment distribution remains unchanged. The results are shown in table 2. midas civils' Initial Tangent Displacement for Erected Structures option is used to estimate the real displacement as well as the rotational angle for the parts put in the next stage. This option enables the installation of new segments tangentially while avoiding any discontinuities.

Table 1

Backward construction stage vs Forward construction stage

Backward Construction Stage Anaysis	Forward Construction Stage Analysis
Backward construction Stage -1	Forward construction stage 7(b)
Moment of L-Girders for single tower(not connected at mid-span)	Moment (Ton*m) of L-Girders for single tower(not connected at mid-span)
Deflection profile of the L-Girder	Deflection profile of the L-Girder
Backward construction stage-7(b)	Forward construction stage-1(b)

General Considerations and Uncertainties

A cable-stayed bridge construction stage analysis begins with a linear analysis that takes into account the impacts of developing the structure in stages, as well as the exact loading situation for each step. Creep and shrinkage must be evaluated since both time dependent effects and non-linearity impact structural performance. Furthermore, the temperature at the construction site may have an impact on the structural components.

Time Dependent Effects

The stress and strain experienced by reinforced or prestressed concrete structures fluctuate over time due to creep, shrinkage of concrete, and relaxation of the steel used for pre-stressing. Concrete can develop progressive strain over time as a result of prolonged tension, a phenomenon known as creep (Midas Bridge, n.d.). The age of the concrete during loading and the amount of time that passes following loading have an impact on the amount of immediate strain and creep. Furthermore, if pre-stressed steel is exposed to stresses greater than 50% of its strength, it may also experience creep. Stress levels in service settings can range from 0.5 to 0.8 of the steel's strength, which causes relaxation—a progressive reduction in stress over time (Svensson, 2012). When examining the deformation behavior of prestressed concrete members, this relaxation phenomena is important (Gautam, 2019).

Creep and Shrinkage for Construction Stage Analysis

The time-dependent effects of creep and shrinkage play a considerable influence in the overall geometry of a concrete or composite cable-stayed bridge. Consequently, it is crucial to incorporate the final stress state of the completed bridge into the analysis (Arzoumanian et al., 2016). Both the load history and the casting sequence must be included to achieve an accurate construction stage analysis. To generate accurate estimates of the ultimate stress distribution and profile, each individual building step must be represented in the erection analysis. To produce correct results, the weight of the deck pieces and the equipment used in the building process must be precisely modelled. The weight of a deck section should be separated into its numerous components and progressively added based on the desired construction cycle. By considering the weight distribution and its incremental addition during each stage, a more precise analysis can be conducted (Gautam, 2019). Overall, the construction stage analysis of concrete or composite cable-stayed bridges necessitates the inclusion of time-dependent effects such as creep and shrinkage. Additionally, it requires careful consideration of the load history, casting sequence, and accurate modeling of the weight distribution of deck segments and equipment, ensuring a comprehensive understanding of the final stress state and geometry of the completed bridge. Creep deformations in a member are influenced by sustained stresses. High-strength concrete experiences less creep compared to lower strength concrete under the same stress (Mohebbi et al., 2022). Creep deformations can be 1.5 to 3.0 times larger than elastic deformations. Around 50% of creep occurs in the first few months, with the majority happening within approximately 5 years (Chen & Duan, 2014).
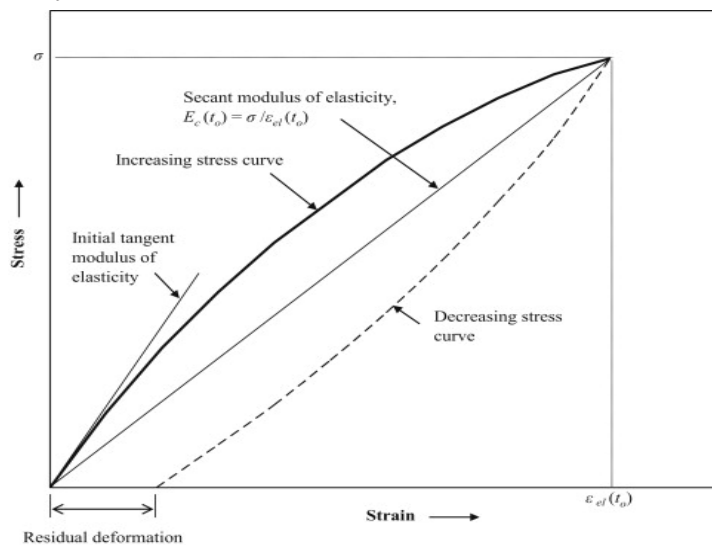
Figure 7

Component of deformation for time dependent concrete (Mohebbi et al., 2022)
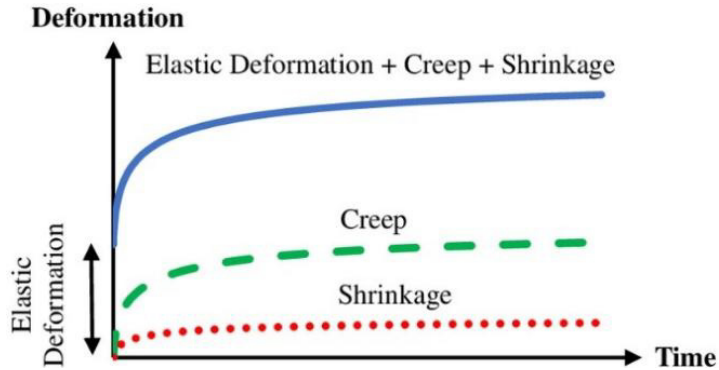
Prestressed girder segments can be pre-tensioned or post-tensioned. In pre-tensioning, the tendon is stretched and anchored in the concrete form before casting. After the concrete gains strength, the tendon is cut, causing a compressive force in the concrete and shortening of the member. Slip may occur at the end. In post-tensioning, the tendon is placed in a duct before casting. Once the concrete reaches the required strength, the tendon is tensioned and anchored at both ends. The duct is then filled with cement mortar. There is a strain incompatibility between the steel and concrete during tensioning, but it does not result in immediate loss of prestress. Except when the tendon is purposefully left unbonded, when strain incompatibility is often disregarded in practical calculations, a complete connection is assumed between the tendon, grout, duct, and concrete following transfer (Ghali et al., 2012).
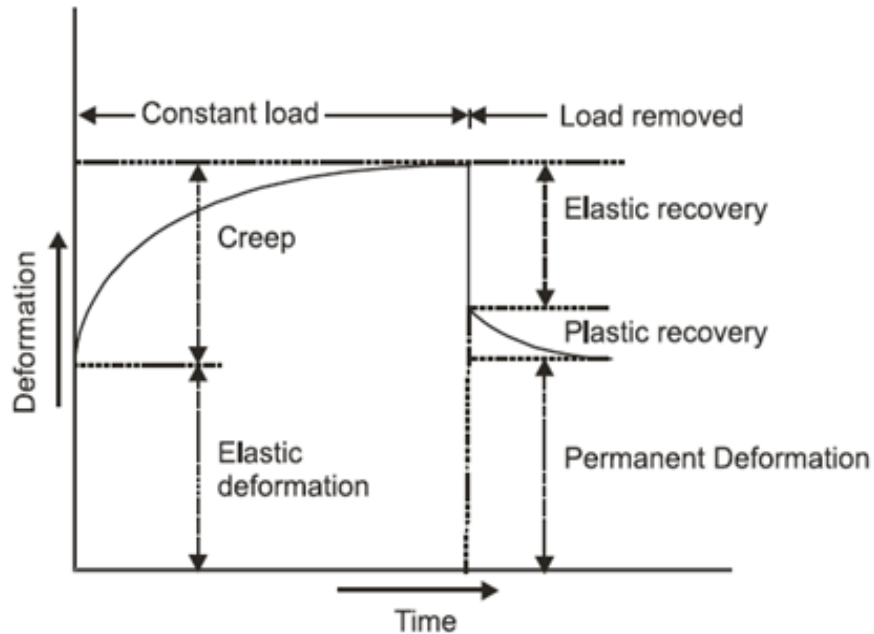
Figure 8

Stress strain curve for concrete

Figure 9

Creep of concrete under the effect of sustained stress

The strain that happens when stress is applied is known as instantaneous strain, and it is stated as follows:

$$\varepsilon_{el}(t, t_0) = \frac{\sigma_c(t_0)}{E_c(t_0)} \tag{1}$$

Top of Form

where $\sigma_c(t_0)$ is the concrete stress and $E_c(t_0)$ is the modulus of elasticity of concrete at age t_0, the time of application of the stress.

Under sustained stress, the strain increases with time due to creep and the total strain – instantaneous plus creep – at time t.

$$\varepsilon(t, t_0) = \frac{\sigma_c(t_0)}{E_c(t_0)} * [1 + \varphi(t, t_0)] \quad , \text{(Shrinkage is neglected)} \tag{2}$$

where $\varphi(t, t_0)$ is a dimensionless coefficient, and is a function of the age at loading, t_0 and the age t for which the strain is calculated. The ratio of creep to instantaneous strain is represented by the coefficient φ, and its value rises as age at loading t_0 decreases and the duration of the stress-sustaining time $(t - t_0)$ grows (Ghali et al., 2012).

Shrinkage is a function of time and is unaffected by stress in the concrete part.

Therefore, the shrinkage can be generally expressed as:

$$E_{sh}(t,t_0) = \varepsilon_{sh0} * f(t,t_0) \tag{3}$$

Where, ε_{sh0} represents the shrinkage coefficient at the final time, $f(t,t_0)$ is a function of time and t stands for the time of observation and t_0 for the initial time of the shrinkage.

Different formulae are created for the prediction of creep in practice codes, based on a product or summation method. For example, in the summation approach of the CEB-FIP 1990 suggests, the total strain at time t, $E_c(t)$, of the concrete member uniaxially loaded at time t_0 with a constant stress $\sigma_c(t_0)$ may be expressed as follows(Comité Euro International du Béton - CEB-FIP, 1993):

$$\varepsilon_c(t) = \varepsilon_{cr}(t_0) + \varepsilon_{cc}(t) + \varepsilon_{cs}(t) + \varepsilon_{cT}(t) = \varepsilon_{c\sigma}(t_0) + \varepsilon_{cn}(t) \tag{4}$$

Where,

$\varepsilon_{ci}(t_0)$ is the initial strain at loading, $\varepsilon_{cc}(t)$ is the creep strain at time $t > t_0$, $\varepsilon_{cs}(t)$ is the shrinkage strain, $\varepsilon_{cT}(t)$ is the thermal strain, $\varepsilon_{c\sigma}(t)$ is the is the stress dependent strain: $\varepsilon_{c\sigma}(t) = \varepsilon_{ci}(t_0) + \varepsilon_{cr}(t)$, $\varepsilon_{cn}(t)$ is the stress independent strain: $\varepsilon_{cn}(t) = \varepsilon_{cs}(t) + \varepsilon_{cT}(t)$.

CEB-FIP 90 Model(Comité Euro International du Béton - CEB-FIP, 1993)

Creep is a time-dependent phenomenon where deformations occur under sustained loads, independent of additional loads. It not only increases deformations but also has an effect on tendon pre-stressing and overall structural behavior. A temporal history of stresses and creep coefficients for different loading ages is required in order to appropriately account for time-dependent variables. Therefore, regulating the construction stages of concrete or composite bridges requires more than just backward analysis. Since creep is a non-mechanical deformation, unless restrictions are placed, deformations may occur without concomitant forces.

The total strain at time t, $E_c(t)$, of the concrete member uniaxially loaded at time t_0 with a constant stress $\sigma_c(t_0)$ may be expressed as follows:

$$\varepsilon_c(t) = \varepsilon_{cr}(t_0) + \varepsilon_{cc}(t) + \varepsilon_{cs}(t) + \varepsilon_{cT}(t) \tag{5}$$

Assumptions and related basic equations for creep

Within the range of service $|\sigma_c| < 0.4f_{cm}(t_0)$, creep is assumed to be linearly related to stress.

For a constant stress applied at time t_0 this leads to

$$\varepsilon_{cc}(t,t_0) = \frac{\sigma_c(t_0)}{E_{ci}} \emptyset(t,t_0) \tag{6}$$

Where,

$\emptyset(t,t_0)$ is the creep coefficient, E_{ci} is the modulus of elasticity at the age of 28 days

The stress dependent strain $\varepsilon_{c\sigma}(t,t_0)$ may be expressed as

$$\varepsilon_{c\sigma}(t, t_0) = \sigma_c(t_0)\left[\frac{1}{E_c(t_0)} + \frac{\emptyset(t, t_0)}{E_{ci}}\right] = \sigma_c(t_0)J(t, t_0) \tag{7}$$

Where, $J(t, t_0)$ is the creep function or creep compliance, representing the total stress dependent strain unit stress, $E_c(t_0)$ is the modiulus of elasticity at the time of loading t_0; Hence, $1/E_c(t_0)$ represents the initial strain per unit stress at loading.

For variable stresses or strains, the principle of superposition is assumed to be valid. On the basis of the assumption and definitions given above the constitutive equation for concrete maybe written as

$$\varepsilon_c(t) = \sigma_c(t_0)J(t, t_0) + \int_{t_0}^{t} J(t, \tau)\frac{\delta\sigma_c(\tau)}{\delta\tau} + \varepsilon_{cn}(t) \tag{8}$$

The application of the principle of superposition is consistent with respect to the assumption of linearity. However, due to actual non-linear behavior of concrete some prediction errors are inevitable when linear superposition is applied to creep of concrete under variable stress particularly for loading or decreasing strains, respectively.
The creep coefficient can be calculated from

$$\phi(t, t_o) = \phi_o\beta_c(t - t_o) \tag{9}$$

where, ϕ_o is the notational creep coefficient, β_c is the coefficient to describe the development of creep with time after loading, t is the age of concrete (days) at the moment considered, t_o is the age of the concrete at loading (days) adjusted according to equation.
The notational creep coefficient can be estimated from

$$\phi_0 = \phi_{RH}\beta(f_{cm})\beta(f_0) \tag{10}$$

With,

$$\phi_{RH} = 1 + \frac{1 - \frac{RH}{RH_0}}{0.46\left(\frac{h}{h_0}\right)^{1/3}} \tag{11}$$

Where,
RH is the relative humidity of the ambient environment (in %), $RH_0 = 100\%$, $h = 2A_c/u$, h is the notational size of the member(mm), where A_c is the cross-section and u is the perimeter of the member in contact with the atmosphere, $h_0 = 100mm$

$$\beta(f_{cm}) = \frac{5.3}{(f_{cm}/f_{cm0})^{0.5}} \tag{12}$$

Where, f_{cm} is the mean compressive strength of concrete at the age of 28

days(MPa), $f_{cm0} = 10MPa$

The adjusted time t_0 is given by:

$$t_{0,T} = \sum_{i=1}^{n} \Delta t_i . exp \left[13.65 - \frac{4000}{273 + T\left(\Delta t_i\right)/T_0} \right] \tag{13}$$

$t_{0,T}$ is the adjusted concrete age which replaces t in the corresponding equations, Δt_i is the number of days where a temperature T prevails $T(\Delta t_i)$ is the temperature the time period (°C) during the time period Δt_i, $T_0 = 1$°C.

The effect of the type of cement on the creep coefficient of the concrete may be taken into account by using the modified as of loading.

$$t_{0,adj} = t_{0,T} \left[\frac{9}{2 + \left(t_{0,T}/t_{1,T}\right)^{1.2}} + 1 \right] \geq 0.5 days \tag{14}$$

Where,

$t_{0,T}$ is the age of concrete at loading (days) adjusted according to equation, $t_{1,T} = 1\ day$ ∝=-1 for slowly hardening concrete SL,

   =0 for normal or rapid hardening cements N and R and

   =1 for rapid hardening high strength cements RS

With,

$$\beta(t_0) = \frac{1}{0.1 + \left(t_{0,adj}/t_1\right)^{0.2}} \tag{15}$$

Now, The development of creep with time is

$$\beta_c(t - t_0) = \left[\frac{(t - t_0)/t_1}{\beta_H + (t - t_0)/t_1} \right]^{0.3} \tag{16}$$

With,

$$\beta_H = 150 \left\{ 1 + \left(1.2 \frac{R_H}{R_{Ho}} \right)^{18} \right\} \frac{h}{h_0} + 250 \leq 1500 \tag{17}$$

Where, $t_1 = 1\ day$, $RH_0 = 100\%$, $h_0 = 100mm$

Validation Example

Midas civil provides the capability to incorporate creep and shrinkage in construction stage analyses. This chapter offers a brief introduction to utilizing these functions in calculations, including a simple verification analysis. The Time Dependent Material Function or pre-existing creep and shrinkage models may be used to determine creep and shrinkage parameters. The Time Dependent Material Link is used to establish

the link between time-dependent material attributes and material data. Each stage's actual erection time may be described in a construction stage analysis, and any changes in load application timing or extra loads can be compensated for via additional stages within the stage (Midas Bridge, n.d.). In construction stage analysis, the behavior of creep can be accommodated by creating additional steps within a stage on a logarithmic scale using the Auto Generation option. These additional stages are created automatically, and the user may choose the number of days for each step to record load variations over a specified time period. The age of activation is specified in the Construction Stage Analysis Data to indicate the impacts of creep and shrinkage on components, signifying the time passed between concrete casting prior to the commencement of the current stage. The age of an element group signifies the duration between concrete casting and the removal of falsework/formwork, indicating when the elements are loaded, particularly for horizontal members such as segments. The structural system which is analyzed for the validation of the creep and shrinkage is as shown in figure 10.

Figure 10

Validation example for creep and shrinkage
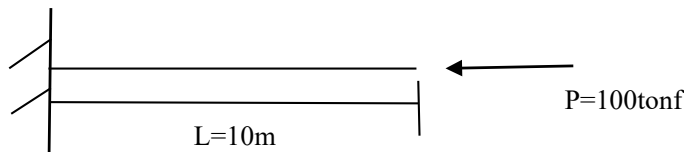
Table 2

Input data of the validation model

Data	Value
Area (A)	1.00 m^2
Stiffness (I)	0.08333 m^4
Poisson Ratio (μ)	0.18
Modulus of elasticity (E)	3.63*10^6 tonf/m^2

Table 3

Data for defining the creep and shrinkage model

Creep and shrinkage data	
Code	CEB-FIP
Compressive strength of concrete at the age of 28 days	4000 tonf/m²
Relative Humidity	80%
Notational size of member	0.5

Age of concrete at the beginning of shrinkage	3 days
Age of concrete at the beginning of loading	10 days

Figure 11

Creep coefficient and shrinkage strain defined in midas civil
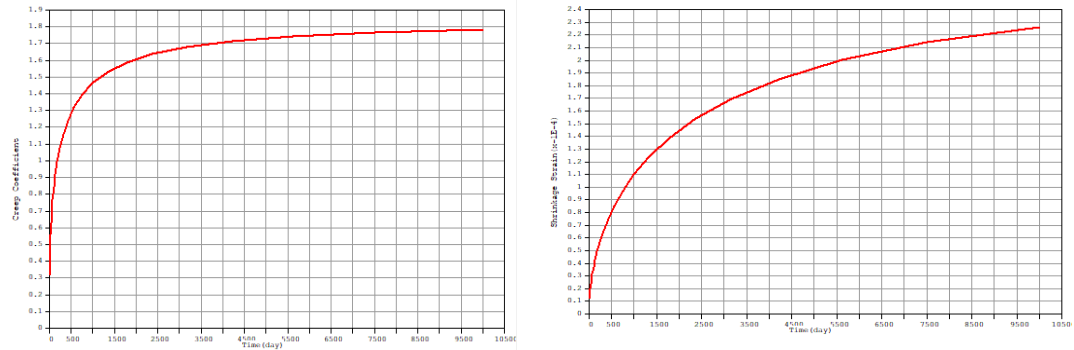
The cantilever is represented by a single element that is activated during the initial construction stage. At an age of 7 days, the first load (P1) of 100 tonf is applied. After 60 days, the second construction stage begins and a second load (P2) of 100 tonf is activated. In the third construction stage, which starts after 180 days, a third load (P3) of 100 tonf is applied. The total simulation duration is 460 days. The elastic shortening of the cantilever due to a single load is approximately 0.2755 mm. For the abovementioned system the analysis is done in the midas and for the manual calculation formulas from the CEB-FIP Model 1990 are used to calculate the total creep. The calculated axial creep deformation for each construction stage is given in the table 4.
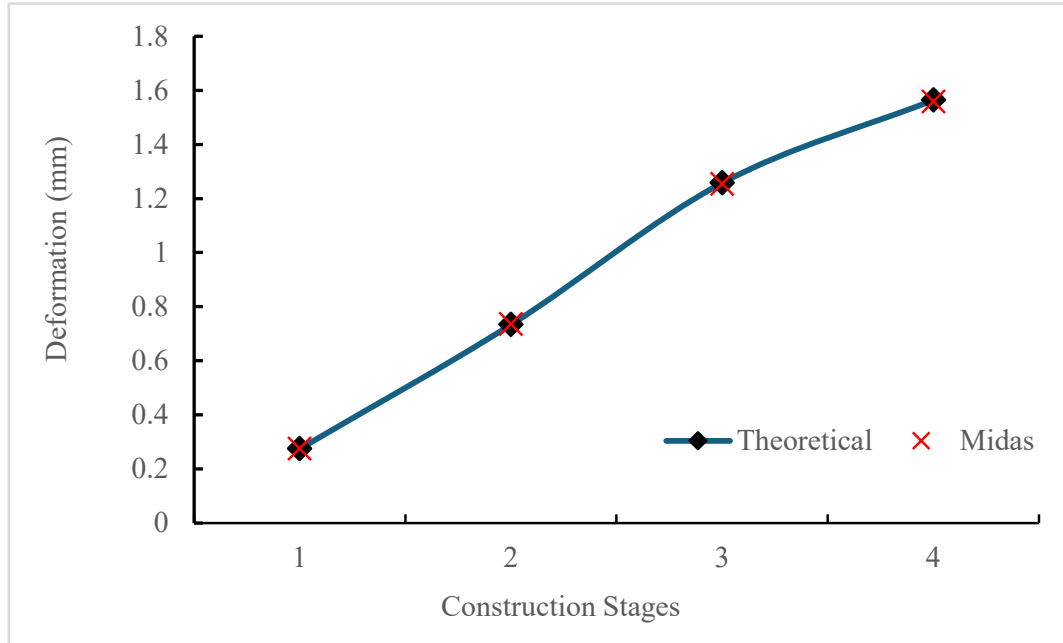
Table 4

Comparison of the results from standard calculation and midas software

Construction stage	Results (ΔL) (mm)		
	Theoretical	midas	Difference
CS-1	0.275	0.275	0%
CS-2	0.734	0.736	0.27%
CS-3	1.258	1.254	0.32%
CS-4	1.564	1.559	0.32%

Figure 12

Comparison of the results from standard calculation and midas civil software

For the creep value after 180 and 460 days, the difference between the theoretical and the midas civil value is 0.32%, as shown in figure 12, which is tolerable.

Structural Detailing

The bridges under analysis were a representative of typical bridge design that have been pre-determined. To evaluate this bridges, various analytical methods are employed, referenced from a range of literature sources. The Cable Stayed Bridge has a main span of 122m with 60m long side spans. The deck of Bridge consists of a steel composite section with an A-shaped RCC pylon having legs supported on the pile cap. Inverted Y-shaped pylons are used for the bridge to transfer the forces from the stay cables. Due to the cable's arrangement, the Pylon height was adjusted to get a minimum clearance of 5.50m over the deck slab. At location P16, an inverse Y-shaped pylon with two legs was provided, while at P17, the pylon was an inverse Y-shaped with four legs from where loads are transferred to the foundation.
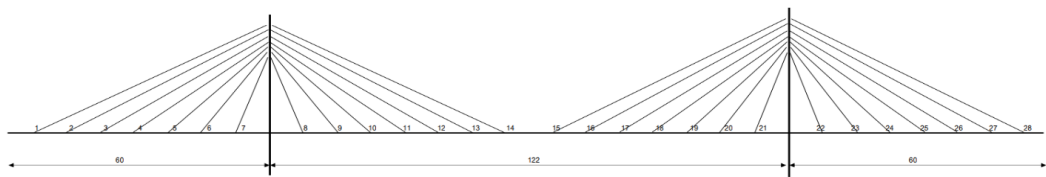
Table 5

Material Properties of the bridge

Particulars	Grade of Concrete	Grade of Steel
Deck Slab	M50	Fe500
Pylon	M50	Fe500
Pile Cap	M45	Fe500
Pile	M35	Fe500
Steel Girder		E-330(Fe-490)

Figure 13

Structural arrangement of cable-stayed bridge

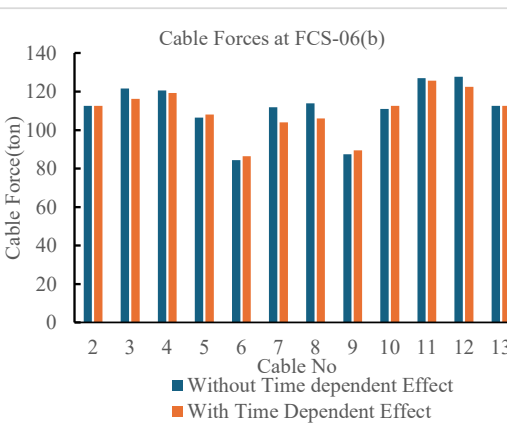**Comparison of forward construction stage analysis with time dependent material properties and with normal Condition**

Comparison of Cable Forces

Figure 14

Comparison of Cable forces for each construction stage with and without considering time-dependent material property

Cable Forces at FCS-03(b)

Cable Forces at FCS-04(b)

Cable Forces at FCS-05(b)

Cable Forces at FCS-06(b)

Cable Forces at FCS-07(b)
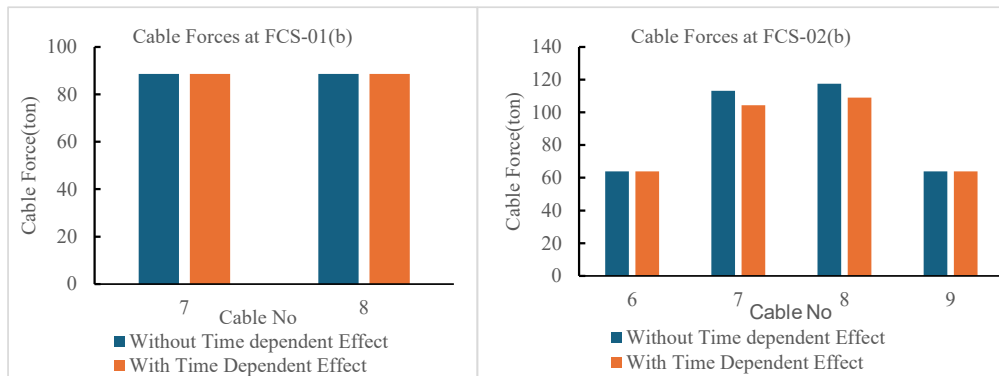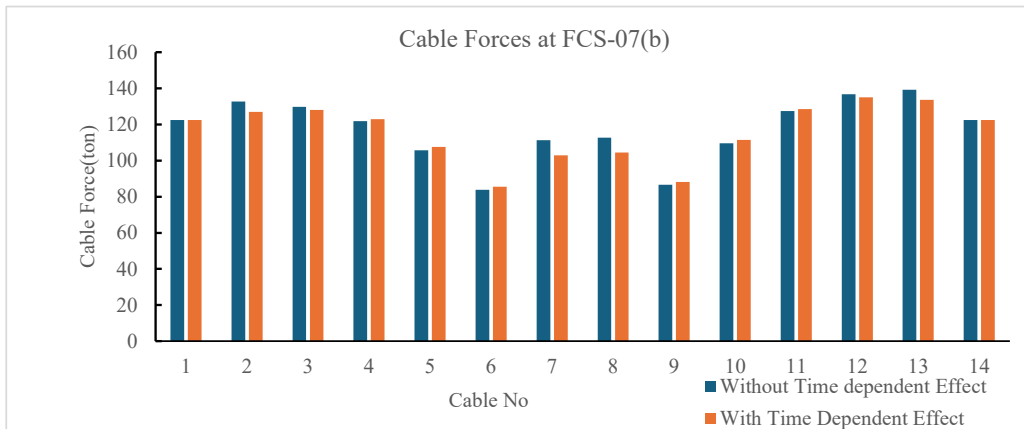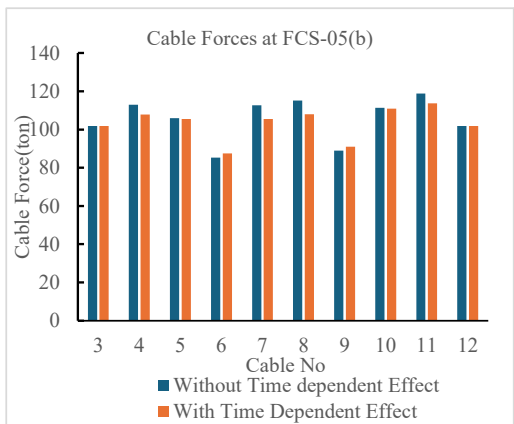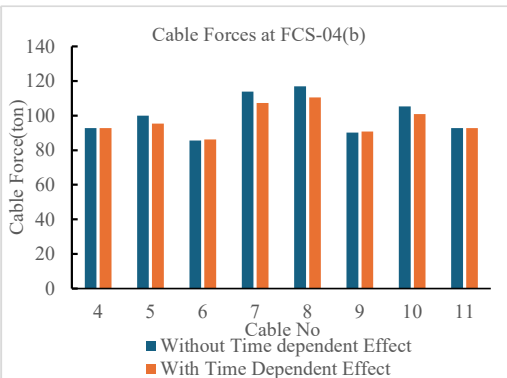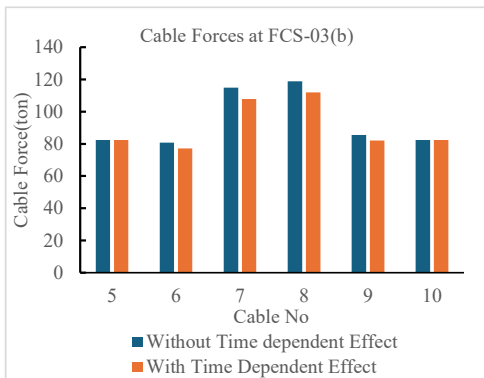
Comparison of Deflection

Deflection of the bridge depends on the loading on the bridge and initial pretension that has been provided. The results that are.

Table 6

Maximum deflection of the L-girder

Construction Stage	Maximum Deflection (mm)		Difference(mm)
	Time-dependent	Normal	
FCS-01(b)	-7.45	-7.17	4%
FCS-02(b)	-15.16	-13.42	13%
FCS-03(b)	-17.41	-15.62	11%
FCS-04(b)	-18.99	-17.33	10%
FCS-05(b)	-20.16	-18.53	9%
FCS-06(b)	-21.32	-19.67	9%
FCS-07(b)	-24.96	-21.38	17%

Comparison of Bending Moment

Table 7

Comparison of maximum Moment Considering material Time-dependent material property and without.

Construction Stage		Maximum Moment (Ton*m)		Difference (%)
		Time-dependent	Normal	
FCS-01(b) (168 days)	Sagging	115.44	115.36	0%
	Hogging	-3.84	-3.84	0%
FCS-02(b) (222 days)	Sagging	50.15	46.4	-7%
	Hogging	-123.48	-128.71	4%
FCS-03(b) (254 days)	Sagging	46.38	45.89	-1%
	Hogging	-139.59	-144.95	4%
FCS-04(b) (286 days)	Sagging	53.71	53.2	-1%
	Hogging	-144.51	-149.86	4%
FCS-05(b) (318 days)	Sagging	57.84	56.73	-2%
	Hogging	-145.2	-150.5	4%
FCS-06(b) (350 days)	Sagging	71.74	70.46	-2%
	Hogging	-145.75	-151.02	4%
FCS-07(b) (382 days)	Sagging	75.1	73.55	-2%
	Hogging	-147.2	-152.42	4%

The results show several key differences in results when considering time-dependent material properties versus normal conditions.

Cable Forces. This result represents there are observable differences (2-5%) in cable forces when accounting for time-dependent properties. These findings are supported

by, Gautam (Gautam, 2019), who emphasized that the sequence of cantilever erection combined with creep effects influences the development of cable forces over time.

Deflection. The maximum deflection of the L-girder shows significant differences between time-dependent and normal conditions. In the final stage (FCS-07(b)), the maximum deflection with time-dependent properties is -24.96 mm, compared to -21.38 mm under normal conditions, a difference of 17%. The differences range from 4% to 17% across various construction stages, with time-dependent analysis consistently showing larger deflections. These findings align well with the observations by Arzoumanis et al. (Arzoumanian et al., 2016), who emphasized that in composite cable-stayed bridges, creep and shrinkage considerably reduce stiffness over time, influencing camber predictions during staged erection.

Bending Moment. Differences are observed in both sagging and hogging moments: For sagging moments, the time-dependent analysis generally shows slightly larger values, with differences ranging from 0% to 7%. For hogging moments, the time-dependent analysis consistently shows lower absolute values, with a consistent 4% difference in later stages. These results are consistent with the findings of Pipinato et al. (Pipinato et al., 2012), who demonstrated that the cantilever erection method induces significant variations in internal forces, particularly when non-instantaneous material properties like creep are accounted for.

Overall, these results indicate that considering time-dependent material properties leads to larger deflections, variations in cable forces, and differences in bending moments, which could have significant implications for the design and long-term performance of the structure.

Conclusion

The study demonstrates the significant impact of time-dependent effects, specifically creep and shrinkage, on the structural behavior of concrete and composite cable-stayed bridges. The comparison between analyses with and without considering time-dependent material properties reveals notable differences in cable forces, deflections, and bending moments across various construction stages.

Key findings include:

1. Cable forces showed variations when time-dependent properties were considered, highlighting the importance of accounting for these effects in design and analysis.
2. Deflections were consistently higher when time-dependent properties were included, with differences ranging from 4% to 17% across construction stages. This underscores the potential for underestimation of deformations if creep and shrinkage are not considered.
3. Bending moments also exhibited differences, particularly in sagging moments, which

were generally higher when time-dependent properties were considered.

These results emphasize the necessity of incorporating creep and shrinkage effects in the construction stage analysis of concrete and composite cable-stayed bridges. Neglecting these time-dependent properties could lead to inaccurate predictions of structural behavior, potentially affecting long-term performance and user comfort.

The study also validates the importance of using advanced modeling techniques, such as those provided by software like midas civil, to accurately predict and account for time-dependent effects in bridge design and construction.

Future research could focus on long-term monitoring of actual bridges to further validate these analytical predictions and refine modeling techniques for time-dependent effects in complex bridge structures.

References

(Arzoumanian et al., 2016) S. G. Arzoumanian, R. G. Burg, and J. Schmid, "Creep and shrinkage in composite cablestayed bridges," *Transportation Research Record*, no. 1290, pp. 21–28, 1991.

(Chen & Duan, 2014) W.F. Chen and L. Duan, *Bridge Engineering Handbook: Construction and Maintenance*, 2nd ed., Boca Raton, FL, USA: CRC Press, 2014.

(Cluley & Shepherd, 1996) N. C. Cluley and R. Shepherd, "Analysis of cablestayed bridges for creep, shrinkage and relaxation effects," *Proceedings of the Institution of Civil Engineers*, vol. 116, no. 3, pp. 453–469, 1996.

(Comité Euro International du Béton - CEB-FIP, 1993) Comité EuroInternational du Béton (CEB), *CEBFIP Model Code 1990: Design Code*, Lausanne, Switzerland: Thomas Telford, 1993.

(Gautam, 2019) T. Bahari Gautam, "Construction stage analysis of cablestayed bridges," M.Sc. thesis, Department of Civil & Environmental Engineering, Tufts University, USA, 2019.

(Ghali et al., 2012) A. Ghali, R. Favre, and M. Elbadry, *Concrete Structures: Stresses and Deformations*, 3rd ed., Boca Raton, FL, USA: CRC Press, 2012.

(Gimsing & Georgakis, 2011) N. J. Gimsing and C. T. Georgakis, *Cable Supported Bridges: Concept and Design*, 3rd ed., Chichester, UK: Wiley, 2011.

(Kim et al., 2017) H. J. Kim, D. H. Won, Y. J. Kang, and S. Kim, "Structural stability of cablestayed bridges during construction," *International Journal of Steel Structures*, vol. 17, no. 2, pp. 443–469, June 2017, doi: 10.1007/s1329601760068.

(Midas Bridge, n.d.) M. S. Troitsky, *CableStayed Bridges: Theory and Design*, 2nd ed., Montreal, Canada: CRC Press, 1990.

(Midas Bridge, n.d.) MIDAS Bridge, "Analysis for Civil Structures," [Online]. Available: https://www.midasbridge.com/en. [Accessed: Jun. 17, 2025].

(Midas Bridge, n.d.) MIDAS Bridge, "Construction Stage Analysis," [Online]. Available: https://www.midasbridge.com/en/solutions/construction-stage-analysis. [Accessed: Jun. 17, 2025].

MIDAS Bridge, (n.d.). *Understanding creep primary & creep secondary*. Available: https://www.midasbridge.com/en/blog/bridge-insight/understanding-creep-primary-creep-secondary. [Accessed: Jun. 17, 2025].

(Mohebbi et al., 2022) A. Mohebbi, B. Graybeal, and Z. Haber, "Timedependent properties of ultrahighperformance concrete: compressive creep and shrinkage," *Journal of Materials in Civil Engineering*, vol. 34, no. 6, pp. 040220671–0402206710, Jun. 2022, doi: 10.1061/(ASCE)MT.19435533.0004219.

(Pipinato et al., 2012) A. Pipinato, C. Pellegrino, and C. Modena, "Structural analysis of the cantilever construction process in cablestayed bridges," *Periodica Polytechnica Civil Engineering*, vol. 56, no. 2, pp. 141–166, 2012, doi: 10.3311/pp.ci.2012-2.02.

(Purohit & Bage, 2017) K. H. Purohit and A. Bage, "Cablestayed bridge analysis," *International Journal of Innovative Research in Science, Engineering and Technology*, vol. 6, no. 7, pp. 14245–14252, July 2017, doi: 10.15680/ IJIRSET.2017.0607216.

(Schlaich, 2001) M. Schlaich, "Erection of cablestayed bridges having composite decks with precast concrete slabs," *Journal of Bridge Engineering*, vol. 6, no. 5, pp. 333–340, 2001 .

(Svensson, 2012) H. Svensson, *CableStayed Bridges: 40 Years of Experience Worldwide*, Berlin, Germany: Ernst & Sohn, 2012.

Appendix

Appendix A: Creep Calculation CEB-FIP 1990

Code: CEB-FIP 1990

Units: As shown in calculation

Compressive Strength of the concrete at the age of 28 days:

$$f_{ck} = 39.2266 \ N/mm^2$$

$$f_{cm} = f_{ck} + 8$$

$$= 39.2266 + 8$$

$$= 47.2266 \ N/mm^2$$

Relative humidity (RH)=80%

Notational size of member(h)=500mm (h=2A$_c$/u)

Age of concrete at the beginning of loading:

$$t_{o,T} = 10 days$$

Age of concrete, t=460 days

Cement constant, $\propto=0$,

$$\phi_{RH} = 1 + \frac{1 - \frac{RH}{RH_0}}{0.46\left(\frac{h}{h_0}\right)^{1/3}}$$

$RH_0 = 100\%$

$h_0 = 100mm$

$$\phi_{RH} = 1 + \frac{1 - (80/100)}{0.46(400/100)^{1/3}} = 1.274$$

$$\beta(f_{cm}) = \frac{5.3}{(f_{cm}/f_{cm0})^{0.5}}$$

$f_{cm0} = 10MPa$

$$\beta(f_{cm}) = \frac{5.3}{(47.2266/10)^{0.5}} = 2.439$$

The effect of the type of cement on the creep coefficient of the concrete taken into account by using the modified as of loading.

$$t_{0,adj} = t_{0,T}\left[\frac{9}{2 + (t_{0,T}/t_{1,T})^{1.2}} + 1\right] \geq 0.5days$$

$$t_{0,adj} = 10\left[\frac{9}{2 + (10/1)^{1.2}} + 1\right]^{\propto} \geq 0.5 \ days$$

$=10\geq 0.5 \ days$

$$\beta(t_0) = \frac{1}{0.1 + \left(t_{0,adj}/t_1\right)^{0.2}}$$

$$= \frac{1}{0.1 + (10/1)^{0.2}}$$

$=0.594$

$$\beta_H = 150\left\{1 + \left(1.2\frac{R_H}{R_{Ho}}\right)^{18}\right\}\frac{h}{h_0} + 250 \leq 1500$$

$$\beta_H = 150\left\{1 + \left(1.2\frac{80}{100}\right)^{18}\right\}\frac{500}{100} + 250 \leq 1500$$

=1359.703 ≤1500

$$\beta_c(t - t_0) = \left[\frac{(460 - 10)/1}{1359.703 + (460 - 10)/1}\right]^{0.3}$$

=0.685

$$\phi_0 = \phi_{RH}.\beta_{fcm}.\beta_{t\theta}$$

=1.254*2.439*0.594

=1.817

The Creep Coefficient

$$\phi(tt'_0) = \phi_0.\beta_c(t - t_0)$$

=1.817*0.685

=1.265

$E = 3.63 * 10^6 \ ton f/m^2 \qquad A = 1 \ m^2 \qquad$ l=10 m $\quad P_i = 100 \ tonf$

$$\sigma = \frac{P_i}{A} = \frac{100}{1} = 100 \ ton f/m^2$$

$$\varepsilon_{el} = \frac{\sigma}{E} = \frac{100}{3.63 * 10^{-5}} = 2.755*10^{-5} \qquad \Delta l_0 = l.\varepsilon_{el} = 10 * 2.755 * 10^{-5} = 0.275 \text{mm}$$

$\phi_{11} = 0 \qquad \phi_{21} = 0 \qquad \phi_{31} = 0 \qquad \Delta l_1 = 1 * \Delta l_0$

$\Delta l_1 = 0.275 mm$

$\phi_{12} = 0.667 \qquad \phi_{22} = 0 \qquad \phi_{32} = 0 \qquad \Delta l_2 = 2 * \Delta l_0 + \phi_{12} * \varepsilon_{el} * 1$

$\Delta l_2 = 0.734 \ mm$

$\phi_{13} = 1.00 \qquad \phi_{23} = 0.648 \quad \phi_{33} = 0 \qquad \Delta l_3 = 2 * \Delta l_0 + (\phi_{13} + \phi_{23}) * \varepsilon_{el} * 1$

$\Delta l_3 = 1.258 \ mm$

$\phi_{14} = 1.217 \qquad \phi_{24} = 0.841 \quad \phi_{34} = 0.662$

$\Delta l_4 = 2 * \Delta l_0 + (\phi_{14} + \phi_{24} + \phi_{34}) * \varepsilon_{el} * 1 \quad \Delta l_4 = 1.564 \ mm$